Published in final edited form as:
J Immunol. 2010 December 15; 185(12): 7614–7622. doi:10.4049/jimmunol.1002760.

TLR9 is Actively Recruited to *Aspergillus fumigatus* Phagosomes and Requires the N-terminal Proteolytic Cleavage Domain for Proper Intracellular Trafficking[1]

Pia V. Kasperkovitz[*,†], **Michael L. Cardenas**[*], and **Jatin M. Vyas**[*,†]

[*]Massachusetts General Hospital, Department of Medicine, Division of Infectious Disease, Boston, MA, 02114

[†]Harvard Medical School, Department of Medicine, Boston, MA, 02115

Abstract

Toll-like receptor 9 (TLR9) recognizes unmethylated CpG DNA and induces innate immune responses. TLR9 activation is a multistep process requiring proteolytic cleavage and trafficking to endolysosomal compartments for ligand-induced signaling. However, the rules that govern the dynamic subcellular trafficking for TLR9 after pathogen uptake have not been established. In this study, we demonstrate that uptake of *Aspergillus fumigatus (Af)* conidia induced drastic spatial redistribution of TLR9 to the phagosomal membrane of *Af*-containing phagosomes but not to bead-containing phagosomes in murine macrophages. Specific TLR9 recruitment to the fungal phagosome was consistent using *Af* spores at different germination stages and selected mutants affecting the display of antigens on the fungal cell surface. Spatiotemporal regulation of TLR9 compartmentalization to the *Af* phagosome was independent of TLR2, TLR4 and downstream TLR signaling. Our data demonstrate that the TLR9 N-terminal proteolytic cleavage domain was critical for successful intracellular trafficking and accumulation of TLR9 in CpG-containing compartments and *Af*-phagosomal membranes. Our study provides evidence for a model in which *Af* spore phagocytosis by macrophages specifically induces TLR9 recruitment to *Af* phagosomes and may thereby mediate TLR9-induced antifungal innate immune responses.

INTRODUCTION

Mammalian TLRs detect microbial products and initiate immune responses to infection. The different members of the TLR family recognize and signal to a broad range of microbial ligands, such as bacterial and fungal cell wall components, bacterial lipoproteins and bacterial and viral nucleic acids (1). The nucleic-acid sensing TLRs, TLR3, 7, 8 and 9, are localized to intracellular compartments whereas TLR1, 2, 4, 5 and 6 are expressed at the plasma membrane (2). TLR activation and signal transduction are regulated by subcellular compartmentalization of receptors and downstream signaling components (3) and the intracellular localization of nucleic acid sensing TLRs appears to facilitate self vs. non-self discrimination (4).

The subcellular localization of TLR9, which engages and signals to unmethylated CpG DNA, is tightly regulated and receptor activation is a multi-step process. TLR9 is translated into the endoplasmic reticulum (ER) in its mature, full-length form and then passes through

[1]JMV was supported in part by NIH K08 AI-057999 and DOM Start-up funds. PVK and MLC were supported by MGH DOM start-up funds.

Corresponding author contact information: jvyas@partners.org, Phone: 617.643.6444, Fax: 617.643.6443.

the Golgi to the endolysosomal compartment where the ectodomain is proteolytically cleaved to generate a functional receptor (5, 6). In the endolysosomal compartment, ligand binding to preassembled TLR9 dimers induces a conformational change that allosterically initiates signal transduction (7). While the truncated form of TLR9 can be found in the endolysosomal compartment of unstimulated cells (5), several reports have indicated that TLR9 trafficking is a highly regulated, dynamic process (8–11). The extent to which there is dynamic movement of TLR9 between subcompartments and the underlying processes regulating TLR9 trafficking remain poorly understood.

Though the best-known ligand for TLR9 is unmethylated bacterial and viral CpG-rich DNA, TLR9 has also been implicated in anti-fungal defense (12, 13). A role for TLR9 in host defense against *Aspergillus fumigatus* (*Af*)[2] has been suggested by experiments in murine models for invasive pulmonary aspergillosis (IPA) and allergic bronchopulmonary aspergillosis (ABPA) where TLR9 modulates the innate immune response in the lung (14). *Af* is a common environmental fungus capable of invasive infection in immunocompromised persons and particularly in patients who have undergone allogeneic hematopoietic stem-cell transplantation (15). In addition, *Af* spore forms, including the asexual conidia, can exacerbate allergic and asthmatic disease (16). Evidence for the importance of innate immune mechanisms in fungal defense is mounting. The fungal β-glucan receptor dectin-1 is essential in pulmonary defense against *Af* (17) and collaborates with TLR2 and TLR4 in providing critical immune signals (12, 18–20). While most studies have focused on the importance of TLR2 and TLR4 in defense against *Af*, a polymorphism study associated increased susceptibility to ABPA with a polymorphism in the TLR9 gene (21) and intranasal CpG had a therapeutic effect during established murine fungal asthma (22). However, the cell biological processes underlying TLR9-mediated *Af* immune responses are still largely unresolved. TLR9-mediated recognition of *Af* DNA by human and murine cells induced proinflammatory cytokines (23), but the intracellular processes that enable *Af* antigen recognition by TLR9 in professional antigen presenting cells remain uninvestigated.

To gain insight into the intracellular fate of TLR9 when immune cells are exposed to *Af* conidia, we investigated the spatiotemporal regulation of TLR9 compartmentalization after phagocytosis of *Af* conidia by murine macrophages. We found that the presence of *Af* phagosomes resulted in a dramatic change of the subcellular distribution of TLR9 to a bright, ring-shaped compartment around the *Af* conidia. TLR9 recruitment was specifically induced by *Af*- but not bead-containing phagosomes, indicating that the composition of the phagocytosed content dictates recruitment of TLR9 to the phagosomal membrane. We demonstrated that *Af*-induced TLR9 recruitment was independent of *Af* spore germination stage. Expression of TLR2, TLR4 and the TLR signaling adapters MyD88 and TRIF were not required for successful *Af*-phagosomal TLR9 recruitment. Further investigation of the requirements for proper intracellular trafficking of TLR9 revealed that the TLR9 N-terminal proteolytic cleavage domain was critical for accumulation of TLR9 in CpG-containing compartments and *Af*-phagosomal membranes.

MATERIALS AND METHODS

Reagents

All products used for cell culture were from Invitrogen (Carlsbad, CA). The CpG phosphorothioate oligodeoxynucleotide 1826 (5′-TCCATGACGTTCCTGACGTT-3′) with

[2]Abbreviations used in this paper: *Af*, *Aspergillus fumigatus*; IPA, invasive pulmonary aspergillosis; ABPA, allergic bronchopulmonary aspergillosis; BafA, bafilomycin A1; BMDC, bone marrow-derived dendritic cell; RAW, RAW264.7; WT, wild type; DIC, differential interference contrast; BMDM, bone marrow-derived macrophages.

Alexa Fluor 647 conjugated to the 3′ end was purchased from Integrated DNA Technologies (Coralville, IA). Ovalbumin Alexa Fluor 488 conjugate (O34781) was purchased from Invitrogen. Dynasore and Bafilomycin A1 were purchased from Sigma.

Cell lines and cell culture

RAW 264.7 (RAW) and HEK293T cells were purchased from ATCC and cultured according to ATCC recommendations. Immortalized bone marrow macrophage cell lines derived from wild-type (WT), TLR2/TLR4-deficient and MyD88/TRIF-deficient mice were a gift from Douglas Golenbock (University of Massachusetts Medical School, Worcester, MA). Immortalized macrophage cell lines were cultured and phenotypically characterized by analysis of macrophage surface marker expression and cytokine expression profile as described previously (24).

Plasmids

The lentiviral pHAGE vector containing CD82 fused at the C-terminus to mRFP1 was described previously (25). The retroviral pMSCV vector containing murine TLR9 fused at the C-terminus to GFP (pMSCV-TLR9-GFP) and plasmids encoding VSV-G and Gag-Pol were a gift from Hidde Ploegh (Whitehead Institute for Biomedical Research, Cambridge, MA). The TLR9 deletion mutant lacking residues 441–470 fused at the C-terminus to GFP (pMSCV-TLR9Δ441–470-GFP) was generated from the pMSCV-TLR9-GFP vector by using quikChange XL site-directed mutagenesis (Agilent Technologies, Santa Clara, CA) using the following primers 5-ACG CTG TCA GAA GCC ACC CCT GAA GAG TGT AAG AAC TTC AAG TTC AAG TTC ACC ATG GAC-3 (forward) and 5-CCG AGA CAG GTC CAT GGT GAA CTT GAA GTT CTT ACA CTC TTC AGG GGT GGC TTC-3 (reverse). The final construct sequence was confirmed by sequencing.

Viral transduction

Lentivirus production and transduction were performed as described previously (25). Retroviral transduction was performed as described (8). Briefly, HEK293T cells were transfected with plasmids encoding VSV-G and Gag-Pol, as well as pMSCV-TLR9-GFP or pMSCV-TLR9Δ441–470-GFP. At 24 h and 48 h after transfection, medium containing viral particles was collected, filtered through a 0.45-mm membrane and added to RAW 264.7 macrophages or immortalized macrophages. The next day, cells were given fresh media and antibiotic selection in 5 μg/ml Puromycin was initiated.

Aspergillus fumigatus (Af) strains, growth and surface labeling

The *Af* strain 293 was a gift from Elefterios Mylonakis (Massachusetts General Hospital, Boston, MA). The *Af* mutant strain Δ*rodA* (26) was a gift from Jean-Paul Latgé (Institut Pasteur, Paris, France) and the *alb1* mutant strain (27) was a gift from K. J. Kwon-Chung (NIAID, NIH). *Af* strains were plated on Sabouraud dextrose agar plates supplemented with 100 μg/ml Ampicillin and grown at 30°C for 3–5 days. Conidia were dislodged from plates by gentle scraping and resuspension in PBS. After two washes in ice-cold PBS, conidia were stored in PBS at 4°C for use within 4 weeks or immediately heat-killed at 100°C for 30 min in a heating block. Swollen conidia were prepared by incubation in RPMI at 37°C for 6h. Resting conidia, swollen conidia and hyphal forms were distinguished by microscopy. To detect surface β1,3-glucan exposure, conidia were then stained with an anti-β-glucan antibody specific for β1,3-glucan (Biosupplies, Inc., Australia) diluted 1:200 in 2%BSA/PBS for 1 hour on a rotator and washed three times with PBS. Then conidia were stained for 1 hour at room temp with anti-mouse Alexa Fluor 488 (Invitrogen) diluted 1:500 into 2%BSA/PBS. *Af* conidia were fluorescently labeled by selectively linking Alexa Fluor 647 succinimidyl ester reconstituted in dimethylformamide (100 mg/mL) to primary amines

located on the conidial surface. After 3 PBS washes, conidia were suspended in 500 μL of PBS, and 3 μg of dye was mixed with the pathogen at 37°C for 30 minutes while shaking for 10 sec every 10 min. The dye-pathogen mixture was then washed again 3 times in PBS and kept on ice and protected from light until imaging experiments.

Confocal microscopy

Spinning-disk confocal microscopy was performed on a Nikon Ti-E inverted microscope equipped with a CSU-X1 confocal head (Yokogawa) that provides scan speeds of up to 2,000 frames per second. A Coherent, 4 W, continuous-wave laser was used as an excitation light source to produce excitation wavelengths of 488 nm, 568 nm and 647 nm. To acquire high quality fluorescence images, a high magnification, high numerical aperture (NA) objective, used for Total Internal Reflection Fluorescence Imaging, was used (Nikon, 100X, 1.49 NA, oil immersion). A piezo stage (Prior Instruments, Rockland, MA) capable of X, Y, Z movement was used for z-stack acquisition. A halogen light source and an air condenser (0.52 NA) were used for bright field illumination a polarizer (Nikon, MEN51941) and Wollaston prisms (Nikon, MBH76190) were used to acquire differential imaging contrast (DIC) images. Images were acquired using an EM-CCD camera (Hamamatsu, C9100-13) capable of acquiring high-resolution images under low light levels with high quantum efficiency. Emission light from the sample was collected after passage through the appropriate emission filters (Semrock, Rochester, NY). Image acquisition was performed using MetaMorph software (Molecular Devices, Downingtown, PA)

Phagocytosis and CpG trafficking experiments

Imaging was performed on cells plated in complete medium into chambered coverglass (Lab-Tek/Nunc, ThermoScientific, Rochester, NY) in a temperature-regulated environmental chamber (In vivo Scientific, St. Louis, MO). Unless noted specifically, experiments were conducted with the *Af*293 wild-type strain. After three washes in PBS, *Af* conidia were introduced to the cells at a 5:1 ratio and live cell-imaging was started immediately. Flash far-red-labeled beads (1 and 5 mm); Bangs Laboratories (Fishers, IN) were washed three times in PBS, introduced to the cells at a 10:1 ratio and incubated for 16h. For phagocytosis inhibition experiments, cells were pre-incubated with 100 μM Dynasore (Sigma) under serum-free conditions for 30 min. Subsequently, cells were co-incubated with conidia in the presence of Dynasore under serum-free conditions for 30 min. After washout cells were kept in complete medium. For CpG trafficking experiments, CpG-Alexa Fluor 647 (1 μM) and/or Ovalbumin Alexa Fluor 488 (100μg/ml) were mixed in pre-warmed medium and added to the cells. After 8 min of incubation, cells were washed twice and time-lapse imaging was started.

Image Analysis

The data are representative of at least three independent experiments in which a minimum of 100 cells were visualized. Raw image data files were processed using Adobe Photoshop in accordance to the Ethical Guidelines for scientific image manipulation as proposed by Rossner et al. (28). Quantitative co-localization analysis was performed in Volocity Version 5.3.2.0 using the colocalization module that computes Pearson's correlation and Manders coefficient for the region of interest. Pixels chosen for quantitative analysis were those that lie in a circumferential ring on the equatorial plane of the phagosome. Pixels that may be associated with vesicles were excluded.

RESULTS

Phagosomes containing *Af* conidia specifically recruit TLR9

We studied the effect of phagocytosis of *Af* resting conidia on the subcellular localization of TLR9 using a stable RAW macrophage cell line expressing TLR9-GFP. As we have previously shown that the tetraspanin CD82 is recruited from the endolysosomal compartment to *Af* and *C. neoformans* phagosomes but not to polystyrene bead-containing phagosomes (29), we stably co-expressed CD82-mRFP1 in these cells for use as a marker of endolysosomal and *Af* phagosomal compartments. We found that the presence of *Af* phagosomes dramatically changed the subcellular distribution of TLR9 from its typical pattern of ER and endolysosomal distribution (5, 8–10, 30) to a bright, ring-shaped compartment around the *Af* conidia that co-localized with CD82 (Fig. 1A). To demonstrate that the recruitment of TLR9 and CD82 was uniform throughout the phagosomal membrane, we imaged serially the entire volume of the phagosome and observed robust recruitment throughout (supplemental movie S1). Additionally, RAW cells expressing either TLR9-GFP or CD82-mRFP1 alone demonstrated similar recruitment as cells expressing both fluorescent proteins (data not shown). To ensure that the *Af* conidia were found within intracellular compartments, we used surface labeling of the fungal pathogen with Alexa Fluor 647 (Fig. 1A). DIC images and fluorescent images confirmed that *Af* conidia resided in phagosomes (full Z stack shown as a movie can be found in the supplement S2). Addition of the fluorescent label to *Af* did not affect its ability to recruit CD82 or TLR9 (data not shown). In sharp contrast to *Af* conidia, phagocytosis of a polystyrene bead regardless of size did not result in enrichment of TLR9 or CD82 around the bead (Fig. 1B), indicating that recruitment of TLR9 is not a result of uptake itself but specifically induced by the content of the phagosome. Uptake of *Af* conidia by macrophages that had previously been exposed to polystyrene beads resulted in specific enrichment of TLR9 and CD82 only around the *Af* conidia but not around the bead (Fig. 1C). The merged images of TLR9 and CD82 showed close apposition of the ring-shaped signals around the *Af* phagosome, confirming that these two proteins are found on the phagosomal membrane. Using time-lapse imaging, the associations remained close throughout the time imaged (data not shown). To determine the extent of overlap of TLR9-GFP and CD82-mRFP1, isolated images of a phagosome were subjected to statistical analysis (Fig. 1D). Pixels capturing fluorescence intensity around the phagosomal membrane were isolated and subjected to quantitative analysis. The identical 387 pixels were included for analysis for both the CD82-mRFP1 and TLR9-GFP signals. Pixels that may be associated the vesicles nearby were excluded for this analysis. The Pearson's correlation for this image was 0.54 and the Manders Coefficients are Mx=0.97 and My=0.99. These data indicate that TLR9-GFP and CD82-mRFP1 are co-localized on the membrane of the *Af*-containing phagosome.

Phagocytosis of *Af* conidia is dynamin-dependent and induces recruitment of TLR9 within 45 min

Phagocytosis was observed as soon as 10 min after exposure of RAW cells to *Af* conidia. We investigated the pathway by which uptake was mediated by pretreatment of the cells with Dynasore, a cell-permeable small molecule that reversibly inhibits the GTPase activity of dynamin1, dynamin2 and Drp1 (31). In the presence of 100 μM Dynasore, macrophage uptake of *Af* conidia was inhibited although the conidia still adhered to the plasma membrane (Fig. 2A). Using time-lapse imaging, we studied the kinetics of conidial uptake and recruitment of TLR9 and CD82 after reversal of inhibition by washout (Fig. 2B). Phagocytic activity was restored 15 min after Dynasore washout and recruitment of TLR9 and CD82 was seen after 45 min. Maximal levels of recruitment were reached 1h after washout (Fig. 2C).

TLR9 recruitment is independent of *Af* conidial viability, spore-germination stage, surface hydrophobin and pigment

Since our bead experiment demonstrated that TLR9 phagosomal recruitment is specific to *Af* conidia, we next wished to investigate if the ability to induce TLR9 recruitment was related to conidial surface properties that change throughout the different *Af* spore stages. During the spore germination process, *Af* conidia undergo an initial period of isotropic expansion associated with the uptake of water and upon the establishment of a polarity axis, a short germ tube emerges and grows into a hypha (32). Conidial swelling during germination increases surface exposure of fungal β-glucans that can trigger the induction of inflammatory responses through the β-glucan receptor Dectin-1 and allow macrophages to distinguish between *Af* spore stages (18, 33–35). To prevent conidial swelling and increased β-glucan exposure from occurring during our experimental conditions, we heat-killed dormant conidia immediately at 100°C for 30 min. When we exposed cells to these heat-killed conidia, recruitment of TLR9 was not impaired (Fig. 3A) compared to what we had seen for conidia that were dormant but viable. Induction of conidial swelling in RPMI for 6h prior to introduction to the cells had no effect on phagocytosis and TLR9 recruitment (Fig. 3B). To confirm that spore germination was induced by this swelling procedure, we microscopically examined the conidia and observed an increase in size (data not shown). In addition, we stained the conidia for β1,3-glucan and in agreement with previously described findings (34, 35), we detected low levels of β1,3-glucan on dormant conidia whereas ~90% of swollen conidia displayed increased β1,3-glucan levels (Supplemental Fig 1). Heat-killing did not affect β-glucan exposure (Supplemental Fig 1). Thus, our results indicate that TLR9 recruitment by *Af* conidia occurs independently of spore germination stage. Strikingly, after overnight incubation with conidia that were dormant but viable at the time of introduction to the cells, we occasionally observed intracellular hyphal forms that retained the ability to recruit TLR9 (Fig. 3C and Supplemental movie 3). Since a low proportion of phagocytosed *Af* conidia can survive, and germinate, within cells (36), it is unclear if germination occurred intracellularly after phagocytosis of the conidia or if the hyphae were phagocytosed after germination. We next examined if removal of the hydrophobic surface layer on dormant conidia that masks their recognition by the immune system would augment TLR9 recruitment. When we exposed cells to dormant conidia from an *Af* mutant *rodA−/−* strain lacking the hydrophobic RodA protein that is covalently bound to the conidial cell wall through glycosylphosphatidylinositol-remnants (26), we did not see a change in the level of TLR9 recruitment (Fig. 3D). Additionally, the conidial pigment melanin protects conidia from oxidative damage by leukocytes and modulates the response to *Af* conidia by shielding fungal PAMPs (37). To determine whether the absence of melanin would affect TLR9 recruitment, we exposed RAW cells to the *Af* mutant *alb1−/−* strain (27) (Fig. 3E). Taken together, while our bead experiment demonstrated that recruitment of TLR9 to the phagosome is dependent on a signal specific to the *Af* conidia, the signal required for TLR9 recruitment appears to be continuously present throughout the different spore stages and selected *Af* mutants.

TLR2 and TLR4 expression and downstream TLR-signaling are not required for TLR9 recruitment to *Af* phagosomes

As TLR2 and TLR4 have been implicated to be critical in the immune response to *Af* (reviewed in (38)) and these receptors are readily recruited from the plasma membrane to microbial phagosomes (39), we hypothesized that the induction of recruitment of TLR9 by *Af* was mediated by signals derived from surface-expressed TLR2 or TLR4 during phagocytosis. To test this hypothesis, we expressed TLR9-GFP and CD82-mRFP1 in immortalized bone marrow macrophage cell lines. As expected, wild-type cells behaved identically as RAW cells (Fig. 4A). Interestingly, when we used cells deficient in both TLR2 and TLR4, phagocytosis of *Af* conidia and subsequent recruitment of TLR9 and CD82 were

not affected (Fig. 4B), indicating that expression of TLR2 and TLR4 is not required for induction of recruitment. To investigate if downstream signaling from any of the TLR-family members was involved in relaying the signal that induces TLR9 recruitment, we next used cells deficient in both MyD88 and TRIF. In these cells, which are completely incapable of all TLR signaling, we still observed robust recruitment of TLR9 and CD82 (Fig. 4C). Thus, our results indicate that TLR9 redistribution to the *Af* phagosome is independent of TLR signaling.

TLR9 accumulation in CpG- or *Af*-containing compartments requires the TLR9 N-terminal proteolytic cleavage motif

Biochemical experiments have demonstrated that the full-length form of TLR9 must undergo proteolytic maturation in the endolysosomal compartment to become a functionally competent receptor to signal in response to CpG (5, 6). We hypothesized that proteolytic cleavage is a requirement for successful TLR9 intracellular trafficking and retention in subcellular compartments. To investigate the role of proteolytic cleavage in TLR9 trafficking to and retention at the *Af* phagosome, we pretreated cells with a specific inhibitor of vacuolar-type H+-ATPase, Bafilomycin A1. Interestingly, when we exposed these cells to *Af* resting conidia, TLR9 recruitment to the *Af* phagosome was impaired although not completely absent (Fig. 5A). In agreement with our previous data (29), recruitment of CD82 was not affected by Bafilomycin A1. There was still some overlap between the TLR9 and CD82 signal in the *Af* phagosomal membrane and in endolysosomal compartments. These data suggested that phagosomal acidification and TLR9 proteolytic cleavage were involved in successful TLR9 recruitment to the *Af* phagosome. To eliminate the involvement of any other cellular effects of Bafilomycin A1 treatment, we constructed a GFP fusion with a deletion mutant that lacks TLR9 residues 441–470. This mutant has been shown to be uncleavable but appeared to have no gross structural alteration in protein structure (6). Strikingly, TLR9Δ441–470 appeared to be exclusively localized to the ER (Fig. 5B). We detected no TLR9Δ441–470 in the *Af* phagosomal membranes whereas CD82 recruitment occurred normally. There was no overlap between the CD82 and TLR9Δ441–470 signals anywhere in the cell and the phagosomal membrane contained exclusively CD82. Because these data demonstrated that the presence of the N-terminal cleavage site was required for accumulation of TLR9 in *Af* phagosomal membranes, we next examined if TLR9 translocation to CpG-containing endolysosomal compartments also required proteolytic cleavage. Translocation of TLR9 from the ER to CpG-containing lysosomal compartments has been demonstrated in various cell types (8, 9, 11). Because we saw robust co-localization of TLR9 and CD82 in *Af* phagosomal membranes, we hypothesized that CD82 also intersects the CpG/TLR9 trafficking pathway in the endolysosomal compartment. When we incubated CD82-mRFP1-expressing RAW cells with fluorescent CpG, we found that CpG was endocytosed into a CD82-negative compartment and rapidly redistributed to a CD82-positive compartment (Fig. 6A, first three panels). Within 30 min. all CpG was found in CD82-positive compartments that co-stained with lysosomal markers such as OVA (Fig. 6A, last two panels) and other lysosomal markers such as DQ-OVA and Lysotracker (data not shown). To verify that the CpG/CD82 compartment is the site where TLR9 is recruited, we expressed TLR9-GFP and CD82-mRFP1 in RAW cells and exposed these cells to fluorescent CpG. As anticipated, we observed rapid recruitment of TLR9 to CpG-containing, CD82-positive compartments (Fig. 6B). In stark contrast, TLR9Δ441–470 was not recruited to CpG-containing compartments although CpG trafficking to CD82-positive compartments occurred normally (Fig. 6B). There was no overlap between the CD82 and TLR9Δ441–470 signals anywhere in the cell and all TLR9Δ441–470 remained in a distinct pattern indicative of the ER. While we cannot know if the deletion mutant TLR9Δ441–470 fails egress from the ER or retention after translocation to post-ER compartments, the absence of the N-terminal cleavage site clearly prevents accumulation of TLR9 in the

endolysosomal/phagosomal compartments containing either CpG and/or *Af*. Therefore, our data demonstrate that TLR9 proteolytic cleavage is a requirement for successful intracellular trafficking and subcellular compartmental retention.

DISCUSSION

The importance of TLR9 trafficking to endolysosomal compartments for receptor functionality and ligand-induced signaling has been well documented (5–9), but exactly how these processes are integrated into the dynamic cellular infrastructure in which TLR9 operates after pathogen uptake has not been established. We have now demonstrated that TLR9 is specifically redistributed to the phagosomal membrane of *Af* spore-containing phagosomes but not bead-containing phagosomes. The TLR9 N-terminal proteolytic cleavage site was a critical requirement for TLR9 recruitment to *Af* phagosomes. Although TLR9 has been implicated in host defense against *Af* (12, 14), the intracellular processes that enable *Af* antigen recognition by TLR9 in innate immune cells remain unclear. To our knowledge, this report is the first to demonstrate that TLR9 specifically accumulates at the fungal phagosome. Selective compartmentalization of pattern recognition receptors to the phagosome may be a requirement for effective orchestration of anti-fungal innate immunity.

TLR9 recruitment to phagosomes was dependent on the content of the phagosome. Indeed, polystyrene beads failed to recruit TLR9 to the phagosomes to levels detectable by fluorescence microscopy. However, the presence of TLR9 in phagosomes has been shown in latex-bead containing RAW cells using biochemical methods (5, 40). Despite the presence of functional TLR9 in latex-bead containing phagosomes, conjugation of beads with CpG did not result in visible enrichment of the total amount of phagosomal TLR9 (5). In sharp contrast, *Af* induced robust recruitment of TLR9 to its phagosome. Moreover, in cells where both *Af* and polystyrene beads were taken up, a clear difference in the level of TLR9 could be visualized. By live cell imaging, we were able to determine that this recruitment occurred within minutes and remained present on the phagosome for hours.

Phagocytosis of *Af* conidia has been shown to require actin polymerization and phosphatidylinositol 3-kinase activity (41). By using Dynasore, a reversible inhibitor of endocytic pathways that blocks coated vesicle formation, we have now demonstrated that GTPase activity of dynamin is an essential step in *Af* conidial phagocytosis. A similar requirement for dynamin activity has been demonstrated for cell entry of the intracellular parasite *Trypanosoma cruzi* (42) and active invasion by *Toxoplasma gondii* (43). While dynamin activity was essential for phagocytosis of both *Af* conidia and beads, TLR9 recruitment after phagocytosis was specific to *Af* conidia. We hypothesized that TLR9 redistribution to *Af*-containing phagosomes involved signaling through another receptor, possibly a plasma membrane localized receptor responding to a component on the *Af* conidial surface. Multiple pattern recognition receptors besides TLR9 have been implicated in the innate immune response to *Af* (12, 18–20, 44–46). A link between the TLR2-mediated recognition of *Af* and the phagocytic response has been suggested (35) and internalization of TLR2 with the *Af* phagosome was shown by microscopy (45). In our search for the receptor mediating the specific recruitment, we demonstrated that expression of TLR2 and TLR4 was not required for *Af*-phagosomal TLR9 recruitment. In addition, TLR9 recruitment occurred normally in the absence of both TLR adaptors MyD88 and TRIF, thereby eliminating the involvement of all downstream TLR signaling in the recruitment process. Our data did not show that deficiency in any of the molecules we analyzed resulted in impaired phagocytosis.

Experiments demonstrating recognition of β1,3-glucan on the *Af* cell wall have suggested that the immune response is tailored towards metabolically active conidia (18, 33) due to preferential recognition by dectin-1 of *Af* swollen conidia that have increased β1,3-glucan

surface exposure (34, 35). However, we observed robust TLR9 recruitment to dormant, heat-killed conidia and did not see a correlation between TLR9 recruitment levels and spore germination stage or increased β1,3-glucan surface exposure. In addition, alterations of the fungal cell wall using mutants of Rod A or melanin synthesis did not perturb the recruitment of TLR9 to the *Af* phagosome. These data suggest that a cell wall component present throughout all developmental stages may mediate TLR9 recruitment. The fungal cell wall is a complex and dynamic structure that contains proteins, glycolipids and polysaccharides that are endowed with distinct immunostimulatory capacities (47). Identification of the component responsible for induction of TLR9 recruitment may significantly enhance our understanding of the innate immune pathways that intracellularly orchestrate antifungal defense.

Maturation of *Af* phagosomes results from fusion with compartments of the endocytic pathway and killing of conidia depends on phagolysosome acidification in alveolar macrophages (41). Our data show that the endolysosomal tetraspanin CD82 intersects the trafficking pathway of TLR9 and marks the compartment where CpG and TLR9 interact. Strikingly, while some TLR9 was already present in the CD82-positive compartment in unstimulated RAW cells, the drastic redistribution of TLR9 to the phagosomal membrane occurred rapidly after *Af* phagocytosis and coincided with recruitment of CD82. It is unclear if the TLR9 molecules recruited to *Af*-containing phagosomes pass through the endolysosome or translocate to the phagosome directly from the ER. Occasionally we observed TLR9/CD82-positive vesicles around the phagosomal membrane that suggested co-delivery of TLR9 and CD82 to the phagosome (Fig. 1D). However, it is possible that TLR9 can reach the *Af* phagosome by both pathways.

Multiple factors have been implicated in TLR9 targeting to subcellular compartments. Delivery of TLR9 to endolysosomal compartments required its interaction with the ER-resident protein UNC93B1, mediated through the transmembrane segment of TLR9 (8). Cytoplasmic targeting motifs controlled TLR9 intracellular localization (48) and the addition of an N-terminal FLAG tag precluded TLR9 ER egress and proteolytic cleavage (5). The importance of the N-terminal cleavage site in TLR9 has been established for its role to generate the functional signaling-competent receptor (5, 6). We have now extended the requirement for the TLR9 N-terminal proteolytic cleavage site for TLR9 accumulation in the endolysosomal and phagosomal compartments. It is unclear if the trafficking defect of the mutant is due to its failure to exit the ER or lack of retention in the endosome or phagosome after translocation. Because successful cleavage of TLR9 required an acidic compartment, it is tempting to speculate that uptake of *Af* conidia and subsequent phagosomal acidification (41) may facilitate cleavage and retention in the phagosome. A recent report indicated that acidification induced by carbohydrates from encapsulated microbes facilitated TLR9 signaling (49). TLR9 recruitment, cleavage and retention at the fungal phasosome may be prerequisite steps for successful signaling to TLR9 ligands that are released during phagosomal processing. Biochemical analyses on *Af*-containing phagosomes are required to resolve the exact spatiotemporal relationship between phagosomal acidification, TLR9 recruitment and TLR9 cleavage.

Our study provides evidence for a model in which *Af* spore phagocytosis by macrophages induces TLR9 recruitment to *Af* phagosomes and may thereby mediate TLR9-induced antifungal innate immune responses. As isolated *Af* nucleic acids activated TLR9 (23), phagosomal TLR9 recruitment may function to enable an immediate response to microbial content released during processing in the phagosome. A similar mechanism has been proposed for *Trypanosoma cruzi* (50). Another possibility is that *Af* spores contain as yet unidentified ligands for TLR9, as the discovery that Malarial Hemozoin acts as a direct ligand for TLR9 demonstrated that TLR9 activation is not limited to nucleic acids (51).

Given the frequent incidence of IPA in immunocompromised patients and severe complications associated with ABPA, it is clear that understanding the molecular mechanisms responsible for triggering innate immune responses to *Af* has both clinical and therapeutic potential, particularly in terms of vaccine development.

Supplementary Material

Refer to Web version on PubMed Central for supplementary material.

Acknowledgments

We thank Douglas Golenbock, Hidde Ploegh, Eleftherios Mylonakis, Jean-Paul Latgé and K. J. Kwon-Chung for kindly providing us with reagents and Lynda Stuart and David Askew for critically reading the manuscript.

References

1. Medzhitov R, Janeway CA Jr. Innate immunity: the virtues of a nonclonal system of recognition. Cell. 1997; 91:295–298. [PubMed: 9363937]
2. Kawai T, Akira S. TLR signaling. Cell Death Differ. 2006; 13:816–825. [PubMed: 16410796]
3. Barton GM, Kagan JC. A cell biological view of Toll-like receptor function: regulation through compartmentalization. Nat Rev Immunol. 2009; 9:535–542. [PubMed: 19556980]
4. Barton GM, Kagan JC, Medzhitov R. Intracellular localization of Toll-like receptor 9 prevents recognition of self DNA but facilitates access to viral DNA. Nat Immunol. 2006; 7:49–56. [PubMed: 16341217]
5. Ewald SE, Lee BL, Lau L, Wickliffe KE, Shi GP, Chapman HA, Barton GM. The ectodomain of Toll-like receptor 9 is cleaved to generate a functional receptor. Nature. 2008; 456:658–662. [PubMed: 18820679]
6. Park B, Brinkmann MM, Spooner E, Lee CC, Kim YM, Ploegh HL. Proteolytic cleavage in an endolysosomal compartment is required for activation of Toll-like receptor 9. Nat Immunol. 2008; 9:1407–1414. [PubMed: 18931679]
7. Latz E, Verma A, Visintin A, Gong M, Sirois CM, Klein DC, Monks BG, McKnight CJ, Lamphier MS, Duprex WP, Espevik T, Golenbock DT. Ligand-induced conformational changes allosterically activate Toll-like receptor 9. Nat Immunol. 2007; 8:772–779. [PubMed: 17572678]
8. Kim YM, Brinkmann MM, Paquet ME, Ploegh HL. UNC93B1 delivers nucleotide-sensing toll-like receptors to endolysosomes. Nature. 2008; 452:234–238. [PubMed: 18305481]
9. Latz E, Schoenemeyer A, Visintin A, Fitzgerald KA, Monks BG, Knetter CF, Lien E, Nilsen NJ, Espevik T, Golenbock DT. TLR9 signals after translocating from the ER to CpG DNA in the lysosome. Nat Immunol. 2004; 5:190–198. [PubMed: 14716310]
10. Leifer CA, Kennedy MN, Mazzoni A, Lee C, Kruhlak MJ, Segal DM. TLR9 is localized in the endoplasmic reticulum prior to stimulation. J Immunol. 2004; 173:1179–1183. [PubMed: 15240708]
11. Yoshizaki M, Tazawa A, Kasumi E, Sasawatari S, Itoh K, Dohi T, Sasazuki T, Inaba K, Makrigiannis AP, Toyama-Sorimachi N. Spatiotemporal regulation of intracellular trafficking of Toll-like receptor 9 by an inhibitory receptor, Ly49Q. Blood. 2009; 114:1518–1527. [PubMed: 19528537]
12. Bellocchio S, Moretti S, Perruccio K, Fallarino F, Bozza S, Montagnoli C, Mosci P, Lipford GB, Pitzurra L, Romani L. TLRs govern neutrophil activity in aspergillosis. J Immunol. 2004; 173:7406–7415. [PubMed: 15585866]
13. Miyazato A, Nakamura K, Yamamoto N, Mora-Montes HM, Tanaka M, Abe Y, Tanno D, Inden K, Gang X, Ishii K, Takeda K, Akira S, Saijo S, Iwakura Y, Adachi Y, Ohno N, Mitsutake K, Gow NA, Kaku M, Kawakami K. Toll-like receptor 9-dependent activation of myeloid dendritic cells by Deoxynucleic acids from Candida albicans. Infect Immun. 2009; 77:3056–3064. [PubMed: 19433551]

14. Ramaprakash H, Ito T, Standiford TJ, Kunkel SL, Hogaboam CM. Toll-like receptor 9 modulates immune responses to Aspergillus fumigatus conidia in immunodeficient and allergic mice. Infect Immun. 2009; 77:108–119. [PubMed: 18936185]
15. Romani L. Immunity to fungal infections. Nat Rev Immunol. 2004; 4:1–23. [PubMed: 14661066]
16. Green BJ, Tovey ER, Sercombe JK, Blachere FM, Beezhold DH, Schmechel D. Airborne fungal fragments and allergenicity. Med Mycol. 2006; 44(Suppl 1):S245–255. [PubMed: 17050446]
17. Werner JL, Metz AE, Horn D, Schoeb TR, Hewitt MM, Schwiebert LM, Faro-Trindade I, Brown GD, Steele C. Requisite role for the dectin-1 beta-glucan receptor in pulmonary defense against Aspergillus fumigatus. J Immunol. 2009; 182:4938–4946. [PubMed: 19342673]
18. Gersuk GM, Underhill DM, Zhu L, Marr KA. Dectin-1 and TLRs permit macrophages to distinguish between different Aspergillus fumigatus cellular states. J Immunol. 2006; 176:3717–3724. [PubMed: 16517740]
19. Dennehy KM, Ferwerda G, Faro-Trindade I, Pyz E, Willment JA, Taylor PR, Kerrigan A, Tsoni SV, Gordon S, Meyer-Wentrup F, Adema GJ, Kullberg BJ, Schweighoffer E, Tybulewicz V, Mora-Montes HM, Gow NA, Williams DL, Netea MG, Brown GD. Syk kinase is required for collaborative cytokine production induced through Dectin-1 and Toll-like receptors. Eur J Immunol. 2008; 38:500–506. [PubMed: 18200499]
20. Ferwerda G, Meyer-Wentrup F, Kullberg BJ, Netea MG, Adema GJ. Dectin-1 synergizes with TLR2 and TLR4 for cytokine production in human primary monocytes and macrophages. Cell Microbiol. 2008; 10:2058–2066. [PubMed: 18549457]
21. Carvalho A, Pasqualotto AC, Pitzurra L, Romani L, Denning DW, Rodrigues F. Polymorphisms in toll-like receptor genes and susceptibility to pulmonary aspergillosis. J Infect Dis. 2008; 197:618–621. [PubMed: 18275280]
22. Ramaprakash H, Hogaboam CM. Intranasal CpG therapy attenuated experimental fungal asthma in a TLR9-dependent and -independent manner. Int Arch Allergy Immunol. 2010; 152:98–112. [PubMed: 20016192]
23. Ramirez-Ortiz ZG, Specht CA, Wang JP, Lee CK, Bartholomeu DC, Gazzinelli RT, Levitz SM. Toll-like receptor 9-dependent immune activation by unmethylated CpG motifs in Aspergillus fumigatus DNA. Infect Immun. 2008; 76:2123–2129. [PubMed: 18332208]
24. Hornung V, Bauernfeind F, Halle A, Samstad EO, Kono H, Rock KL, Fitzgerald KA, Latz E. Silica crystals and aluminum salts activate the NALP3 inflammasome through phagosomal destabilization. Nat Immunol. 2008; 9:847–856. [PubMed: 18604214]
25. Vyas JM, Kim YM, Artavanis-Tsakonas K, Love JC, Van der Veen AG, Ploegh HL. Tubulation of class II MHC compartments is microtubule dependent and involves multiple endolysosomal membrane proteins in primary dendritic cells. J Immunol. 2007; 178:7199–7210. [PubMed: 17513769]
26. Aimanianda V, Bayry J, Bozza S, Kniemeyer O, Perruccio K, Elluru SR, Clavaud C, Paris S, Brakhage AA, Kaveri SV, Romani L, Latge JP. Surface hydrophobin prevents immune recognition of airborne fungal spores. Nature. 2009; 460:1117–1121. [PubMed: 19713928]
27. Tsai HF, Chang YC, Washburn RG, Wheeler MH, Kwon-Chung KJ. The developmentally regulated alb1 gene of Aspergillus fumigatus: its role in modulation of conidial morphology and virulence. J Bacteriol. 1998; 180:3031–3038. [PubMed: 9620950]
28. Rossner M, O'Donnell R. The JCB will let your data shine in RGB. J Cell Biol. 2004; 164:11–13. [PubMed: 18172955]
29. Artavanis-Tsakonas K, Kasperkovitz PV, Papa E, Cardenas ML, Van der Veen AG, Ploegh HL, Vyas JM. CD82 is actively recruited to Cryptococcus neoformans phagosomes and associates with Class II MHC in primary dendritic cells. Submitted for publication.
30. Chockalingam A, Brooks JC, Cameron JL, Blum LK, Leifer CA. TLR9 traffics through the Golgi complex to localize to endolysosomes and respond to CpG DNA. Immunol Cell Biol. 2009; 87:209–217. [PubMed: 19079358]
31. Kirchhausen T, Macia E, Pelish HE. Use of dynasore, the small molecule inhibitor of dynamin, in the regulation of endocytosis. Methods Enzymol. 2008; 438:77–93. [PubMed: 18413242]
32. Harris SD. Cell polarity in filamentous fungi: shaping the mold. Int Rev Cytol. 2006; 251:41–77. [PubMed: 16939777]

33. Steele C, Rapaka RR, Metz A, Pop SM, Williams DL, Gordon S, Kolls JK, Brown GD. The beta-glucan receptor dectin-1 recognizes specific morphologies of Aspergillus fumigatus. PLoS Pathog. 2005; 1:e42. [PubMed: 16344862]
34. Hohl TM, Van Epps HL, Rivera A, Morgan LA, Chen PL, Feldmesser M, Pamer EG. Aspergillus fumigatus triggers inflammatory responses by stage-specific beta-glucan display. PLoS Pathog. 2005; 1:e30. [PubMed: 16304610]
35. Luther K, Torosantucci A, Brakhage AA, Heesemann J, Ebel F. Phagocytosis of Aspergillus fumigatus conidia by murine macrophages involves recognition by the dectin-1 beta-glucan receptor and Toll-like receptor 2. Cell Microbiol. 2007; 9:368–381. [PubMed: 16953804]
36. Wasylnka JA, Moore MM. Aspergillus fumigatus conidia survive and germinate in acidic organelles of A549 epithelial cells. J Cell Sci. 2003; 116:1579–1587. [PubMed: 12640041]
37. Chai LY, Netea MG, Sugui J, Vonk AG, van de Sande WW, Warris A, Kwon-Chung KJ, Jan Kullberg B. Aspergillus fumigatus Conidial Melanin Modulates Host Cytokine Response. Immunobiology. 2009
38. Netea MG, Ferwerda G, van der Graaf CA, Van der Meer JW, Kullberg BJ. Recognition of fungal pathogens by toll-like receptors. Curr Pharm Des. 2006; 12:4195–4201. [PubMed: 17100622]
39. Underhill DM, Ozinsky A, Hajjar AM, Stevens A, Wilson CB, Bassetti M, Aderem A. The Toll-like receptor 2 is recruited to macrophage phagosomes and discriminates between pathogens. Nature. 1999; 401:811–815. [PubMed: 10548109]
40. Shui W, Sheu L, Liu J, Smart B, Petzold CJ, Hsieh TY, Pitcher A, Keasling JD, Bertozzi CR. Membrane proteomics of phagosomes suggests a connection to autophagy. Proc Natl Acad Sci U S A. 2008; 105:16952–16957. [PubMed: 18971338]
41. Ibrahim-Granet O, Philippe B, Boleti H, Boisvieux-Ulrich E, Grenet D, Stern M, Latge JP. Phagocytosis and intracellular fate of Aspergillus fumigatus conidia in alveolar macrophages. Infect Immun. 2003; 71:891–903. [PubMed: 12540571]
42. Barrias ES, Reignault LC, De Souza W, Carvalho TM. Dynasore, a dynamin inhibitor, inhibits Trypanosoma cruzi entry into peritoneal macrophages. PLoS One. 2010; 5:e7764. [PubMed: 20098746]
43. Caldas LA, Attias M, de Souza W. Dynamin inhibitor impairs Toxoplasma gondii invasion. FEMS Microbiol Lett. 2009; 301:103–108. [PubMed: 19817867]
44. Meier A, Kirschning CJ, Nikolaus T, Wagner H, Heesemann J, Ebel F. Toll-like receptor (TLR) 2 and TLR4 are essential for Aspergillus-induced activation of murine macrophages. Cell Microbiol. 2003; 5:561–570. [PubMed: 12864815]
45. Chai LY, Kullberg BJ, Vonk AG, Warris A, Cambi A, Latge JP, Joosten LA, van der Meer JW, Netea MG. Modulation of Toll-like receptor 2 (TLR2) and TLR4 responses by Aspergillus fumigatus. Infect Immun. 2009; 77:2184–2192. [PubMed: 19204090]
46. Mambula SS, Sau K, Henneke P, Golenbock DT, Levitz SM. Toll-like receptor (TLR) signaling in response to Aspergillus fumigatus. J Biol Chem. 2002; 277:39320–39326. [PubMed: 12171914]
47. Bozza S, Clavaud C, Giovannini G, Fontaine T, Beauvais A, Sarfati J, D'Angelo C, Perruccio K, Bonifazi P, Zagarella S, Moretti S, Bistoni F, Latge JP, Romani L. Immune sensing of Aspergillus fumigatus proteins, glycolipids, and polysaccharides and the impact on Th immunity and vaccination. J Immunol. 2009; 183:2407–2414. [PubMed: 19625642]
48. Leifer CA, Brooks JC, Hoelzer K, Lopez J, Kennedy MN, Mazzoni A, Segal DM. Cytoplasmic targeting motifs control localization of toll-like receptor 9. J Biol Chem. 2006; 281:35585–35592. [PubMed: 16990271]
49. Lewis CJ, Cobb BA. Carbohydrate oxidation acidifies endosomes, regulating antigen processing and TLR9 signaling. J Immunol. 2010; 184:3789–3800. [PubMed: 20200279]
50. Bartholomeu DC, Ropert C, Melo MB, Parroche P, Junqueira CF, Teixeira SM, Sirois C, Kasperkovitz P, Knetter CF, Lien E, Latz E, Golenbock DT, Gazzinelli RT. Recruitment and endo-lysosomal activation of TLR9 in dendritic cells infected with Trypanosoma cruzi. J Immunol. 2008; 181:1333–1344. [PubMed: 18606688]
51. Coban C, Igari Y, Yagi M, Reimer T, Koyama S, Aoshi T, Ohata K, Tsukui T, Takeshita F, Sakurai K, Ikegami T, Nakagawa A, Horii T, Nunez G, Ishii KJ, Akira S. Immunogenicity of

whole-parasite vaccines against Plasmodium falciparum involves malarial hemozoin and host TLR9. Cell Host Microbe. 2010; 7:50–61. [PubMed: 20114028]

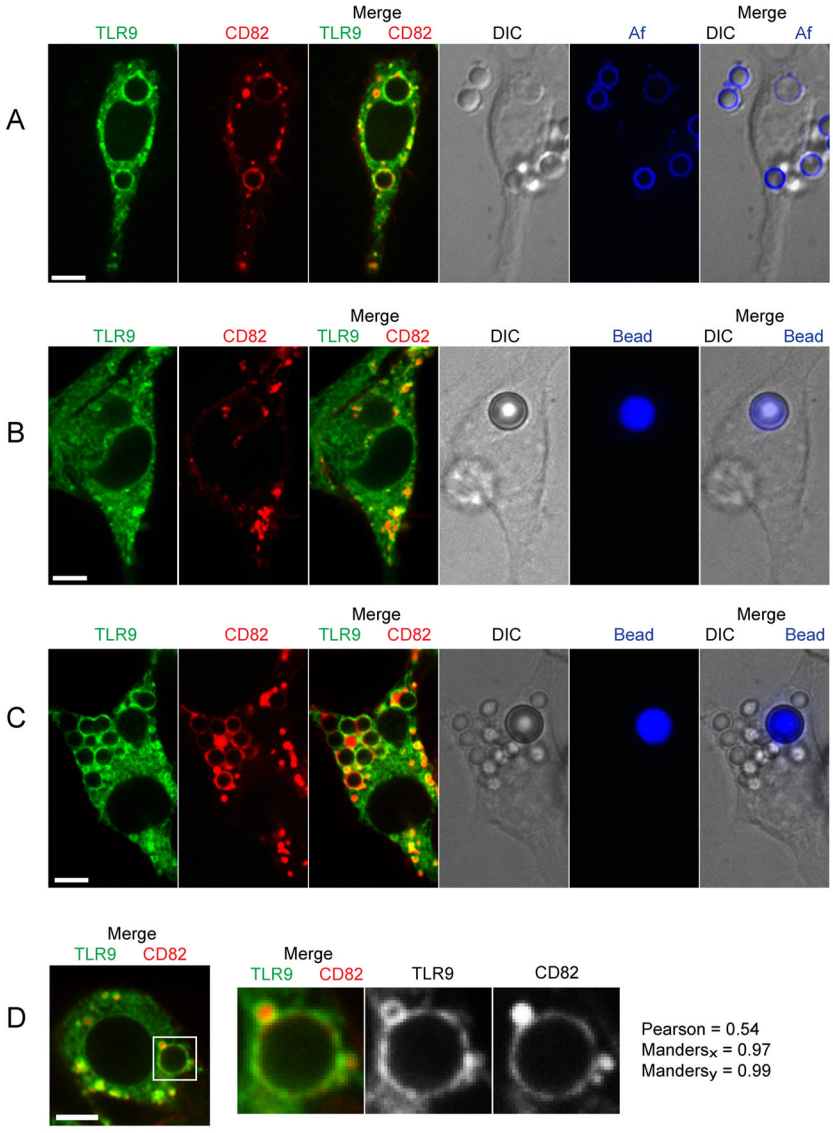

Figure 1. *Af* phagosomes specifically induce recruitment of TLR9

(A–D) Confocal microscopy of RAW macrophages expressing TLR9-GFP (green) and CD82-mRFP1 (red). One focal plane is shown. Scale bar is 5 μm.

(A) Phagosomes containing *Af* resting conidia acquire both TLR9 and CD82. RAW cells were incubated with *Af* resting conidia labeled with Alexa Fluor 647 (blue) for 1 h. Co-localization of TLR9 and CD82 in the phagosomal membrane is apparent in the merged image (third panel); see also supplemental movie S1. The DIC image and the merged DIC/Af (blue) image demonstrate the presence of two labeled *Af* conidia within the cell. See also supplemental movie S2.

(B) Bead-containing phagosomes fail to acquire TLR9 and CD82. RAW cells were incubated for 16 h with Flash far-red-labeled 5 mm beads (blue).

(C) TLR9 is specifically recruited to *Af*-containing phagosomes in cells that have taken up both *Af* resting conidia and polystyrene beads. RAW cells were incubated for 16 h with Flash far-red-labeled 5 mm beads (blue) and then exposed to unlabeled *Af* resting conidia for 1 h. The DIC image demonstrates the presence of unlabeled *Af* conidia within the cell.

(D) Co-localization of TLR9 and CD82 in an *Af*-containing phagosomal membrane. A detail of a representative cell having taken up an *Af* resting conidium was quantitatively analyzed. Pixels associated with large vesicle (10 o'clock position) and 2 smaller vesicles (4 o'clock position) were excluded from this analysis.

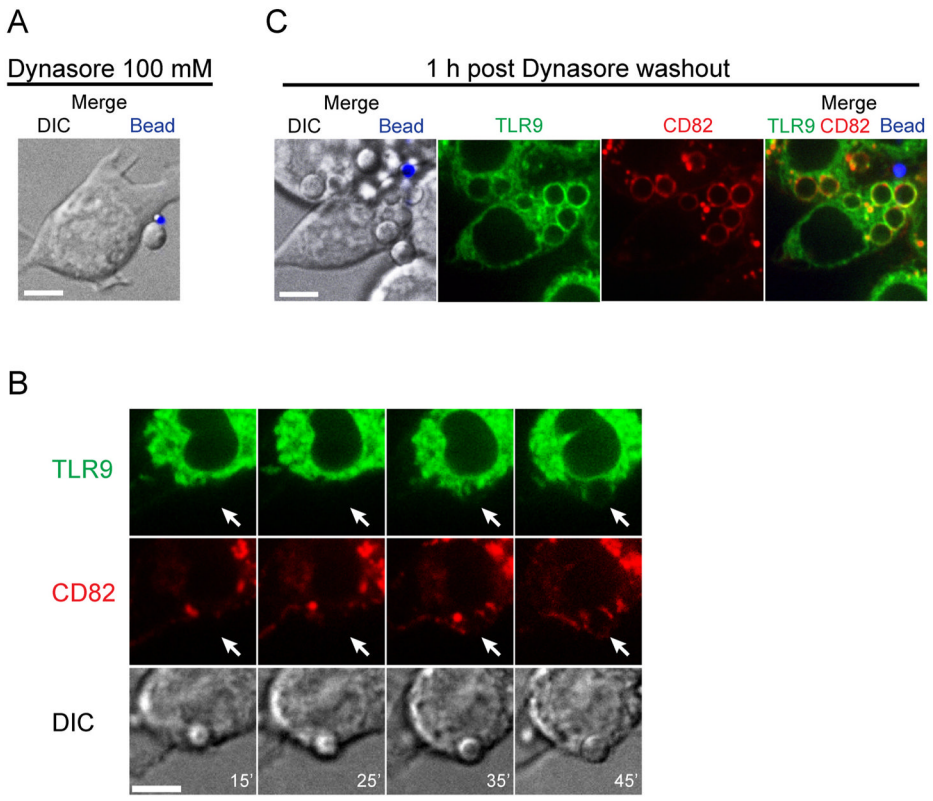

Figure 2. Phagocytosis of *Af* conidia is dynamin-dependent and induces TLR9 recruitment within 45 min

(A–C) Confocal microscopy of RAW macrophages expressing TLR9-GFP (green) and CD82-mRFP1 (red). One focal plane is shown. Scale bar is 5 μm.

(A) The dynamin inhibitor Dynasore blocks uptake of *Af* conidia and polystyrene beads. RAW cells were pretreated with 100 mM Dynasore for 30 min before being exposed to *Af* resting conidia (unlabeled) and 1 μM fluorescent polystyrene beads (blue). The presence of Dynasore did not interfere with adherence of conidia and beads to the plasma membrane.

(B) *Af* phagosomes acquire TLR9 and CD82 within 45 min after reversal of dynamin inhibition by Dynasore washout. Time-lapse images were acquired at indicated times DIC panel, white numbers in lower right corner indicate time (in min.) post washout. The white arrows in the red and green channels show the site of *Af* conidial entry.

(C) Potent recruitment of TLR9 and CD82 to *Af* phagosomes is reached 1 h after Dynasore washout. The merged image on the right shows a representative cell having taken up five unlabeled *Af* resting conidia and one extracellular 1 μM polystyrene bead.

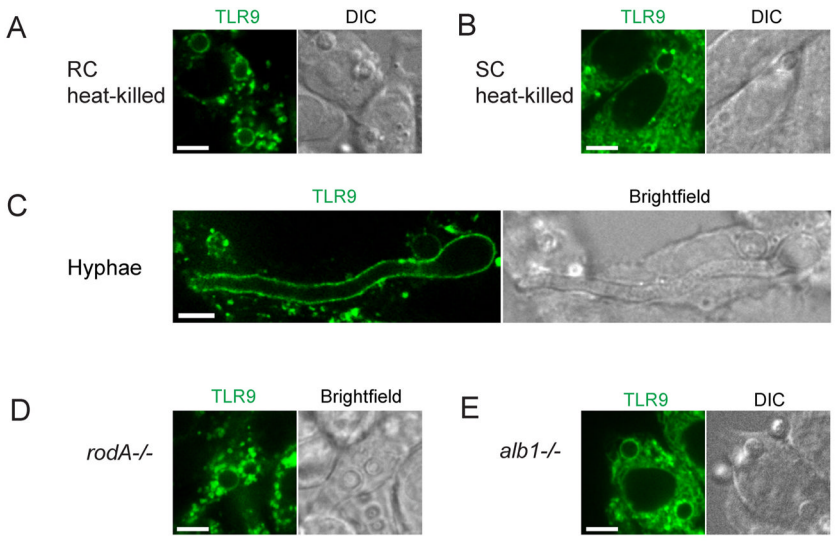

Figure 3. TLR9 recruitment is independent of *Af* spore viability, germination stage, surface hydrophobin and pigment

Confocal microscopy of RAW macrophages expressing TLR9-GFP (green). One focal plane is shown. Scale bar is 5 μm. Wild-type *Af* resting conidia were either heat-killed immediately or swollen for 6h and heat-killed. Resting heat-killed *Af* conidia (A), swollen heat-killed conidia (B) and *Af* hyphae (C) retain the ability to recruit TLR9. See also supplemental movie S3.

Absence of the hydrophobic surface protein RodA (D) or the conidial surface pigment melanin (E) does not interfere with phagosomal TLR9 recruitment by *Af* resting conidia.

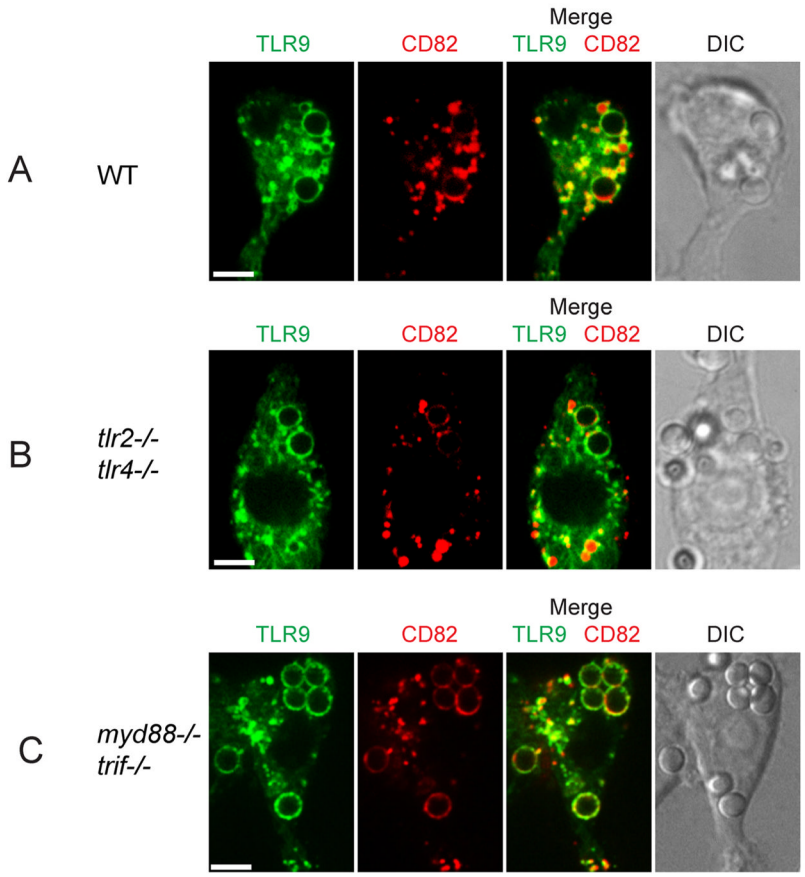

Figure 4. Expression of TLR2 and TLR4 and downstream TLR-signaling are not required for TLR9 recruitment

(A–C) Confocal microscopy of immortalized bone marrow-derived macrophages (BMDM) expressing TLR9-GFP (green) and CD82-mRFP1 (red). One focal plane is shown. Scale bar is 5 μm. Cells were incubated for 1 h with *Af* resting conidia. Representative cells showing phagosomal acquisition of TLR9 and CD82 are shown in wild-type macrophages (A), TLR2/TLR4-deficient macrophages (B) and TLR-signaling incompetent MyD88/TRIF-deficient macrophages (C).

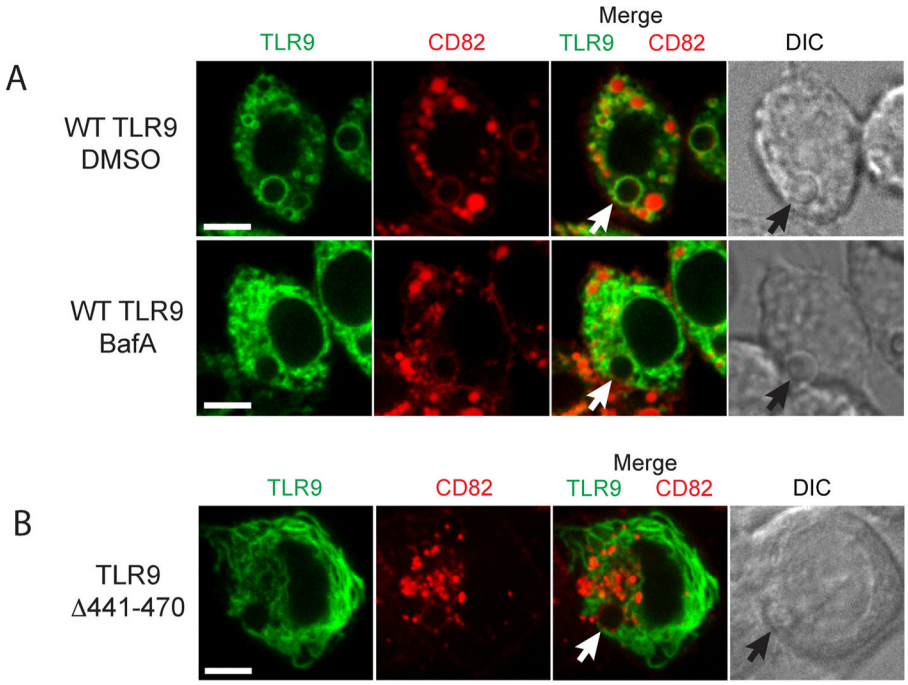

Figure 5. TLR9 accumulation in *Af* phagosomes requires the TLR9 N-terminal proteolytic cleavage motif

(A–B) Confocal microscopy of RAW macrophages. One focal plane is shown. Scale bar is 5 μm.

(A) Blockage of proteolytic cleavage with Bafilomycin A1 results in impaired TLR9 recruitment. RAW cells expressing CD82-mRFP1 (red) and Wild-type TLR9-GFP (green) were pretreated with 100 nM Bafilomycin A1 or DMSO vehicle control for 2 h and then exposed to resting *Af* conidia. Bafilomycin A1 treatment results in impaired recruitment of TLR9 but not CD82 whereas both TLR9 and CD82 recruitment are not affected by the vehicle control (shown by white arrow). The black arrow shows the phagocytosed conidium in DIC image.

(B) TLR9Δ441–470 is not recruited to *Af*-containing phagosomes. RAW cells expressing CD82-mRFP1 and TLR9Δ441–470-GFP were incubated with resting *Af* conidia. TLR9Δ441–470 fails to accumulate on the *Af*-containing phagosome whereas CD82 recruitment is unaffected (shown by white arrow). The black arrow shows the phagocytosed conidium in DIC image.

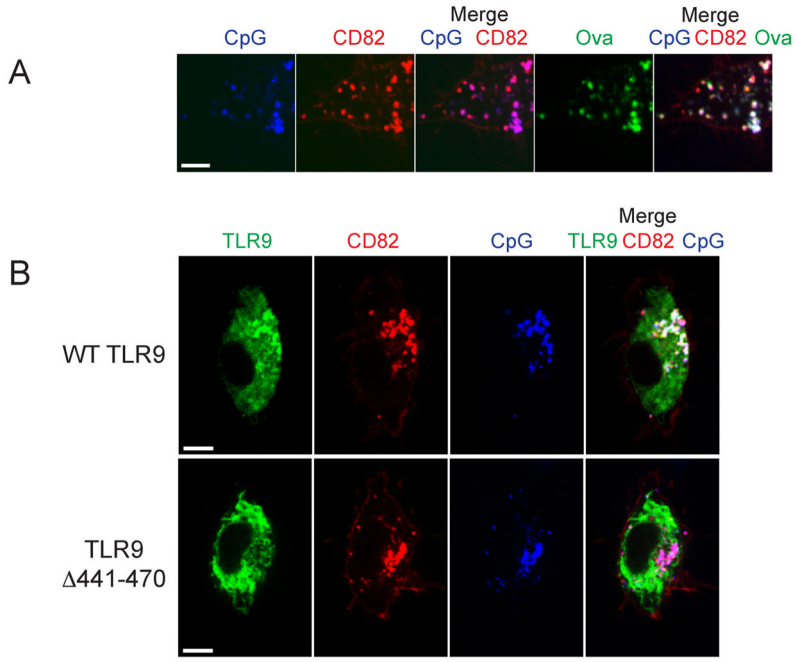

Figure 6. TLR9 accumulation in CpG-containing compartments requires the TLR9 N-terminal proteolytic cleavage motif

(A–D) Confocal microscopy of RAW macrophages. One focal plane is shown. Scale bar is 5 μm.

(A) CpG is redistributed to a CD82-positive endolysosomal compartment within 30 min. RAW cells expressing CD82-mRFP1 (red) were incubated with 1 μM CpG-Alexa Fluor 647 (blue) and ovalbumin (green) for 8 min and then medium was replaced. The merged image shows colocalization of CpG (blue), OVA (green) and CD82 (red) after 30 min.

(B) TLR9Δ441–470-GFP fails to be recruited to CpG-containing compartments. CD82 intersects the TLR9 trafficking pathway and marks the site where Wild-type TLR9 is recruited. RAW cells expressing CD82-mRFP1 (red) and Wild-type TLR9-GFP (green, first series of panels) or TLR9Δ441–470-GFP (green, second series of panels) were incubated with 1 μM CpG-Alexa Fluor 647 (blue) for 8 min and medium was replaced. The merged image shows that 1 h after CpG addition wild-type TLR9 has accumulated in CpG/CD82-positive compartments whereas TLR9Δ441–470 still displays an ER-like distribution. The merged image shows no overlap between TLR9Δ441–470 and the CpG/CD82 double-positive compartment.